within 6 months; for patient A, AST returned to reference range within 6 months and ALT within 7 months (Figure). Because the patients were asymptomatic at the time of rebound, we did not perform liver biopsies.

Each patient had acquired yellow fever in Ilha Grande, Brazil, as had 11 other nonvaccinated travelers to Brazil in 2018 (*3*), before vaccination against yellow fever was recommended for travelers to the states of São Paulo and Rio de Janeiro. For each of the 2 patients reported here, illness was similar: relatively mild disease despite jaundice and severe cytolysis (AST >1,200 IU/L, ALT >1,500 IU/L at diagnosis), known risk factors associated with higher mortality rates (*4*). For each patient, hepatic cytolysis rebounded ≈2 months after the initial peak, with no clinical signs or symptoms and no detection of other pathogens. Previous reports have described liver cytolysis during yellow fever as being acute, decreasing rapidly on days 9–15, then reaching the upper limits of the reference range on day 16, and some persisting up to 2 months (*5*). Liver biopsy results have shown that liver lesions can persist up to 2 months (*6*).

We report persistent hepatitis over 6 months with a rebound of hepatic cytolysis after 2 months. In comparison, relapse has been described for ≈3% of patients with hepatitis A (*7*) with a biphasic peak of ALT (*7,8*) and detection of hepatitis A virus RNA in plasma (*9*), both 4–8 weeks after the first peak.

In terms of the cause of the hepatic cytolysis rebound in the 2 patients reported here, neither had taken a hepatotoxic drug during the rebound period, and results of deep sequencing for eukaryotic pathogens and autoimmune antibodies were negative. However, major yellow fever virus neutralizing activities were detected. Thus, the rebound could be attributed to host immune response to yellow fever virus rather than to another pathogen or to direct effects of the virus itself. In summary, our results show that yellow fever can induce persistent hepatitis with a rebound of liver cytolysis, probably an immune response to the yellow fever virus.

About the Author

Dr. Denis is an infectious diseases clinician working in the tropical and infectious diseases department at St. Louis Hospital, Paris, France. Her research interests focus on epidemiology and infections in immunocompromised patients.

References

1. Mercier-Delarue S, Durier C, Colin de Verdière N, Poveda JD, Meiffrédy V, Fernandez Garcia MD, et al. Screening test for neutralizing antibodies against yellow fever virus, based on a flavivirus pseudotype. PLoS One. 2017;12:e0177882. http://dx.doi.org/10.1371/journal.pone.0177882
2. Naccache SN, Federman S, Veeraraghavan N, Zaharia M, Lee D, Samayoa E, et al. A cloud-compatible bioinformatics pipeline for ultrarapid pathogen identification from next-generation sequencing of clinical samples. Genome Res. 2014;24:1180–92. 10.1101/gr.171934.113 http://dx.doi.org/10.1101/gr.171934.113
3. Oliosi E, Serero Corcos C, Barroso PF, Bleibtreu A, Grard G, De Filippis BAM, et al. Yellow fever in two unvaccinated French tourists to Brazil, January and March, 2018. Euro Surveill. 2018;23. http://dx.doi.org/10.2807/1560-7917.ES.2018.23.21.1800240
4. Tuboi SH, Costa ZG, da Costa Vasconcelos PF, Hatch D. Clinical and epidemiological characteristics of yellow fever in Brazil: analysis of reported cases 1998-2002. Trans R Soc Trop Med Hyg. 2007;101:169–75. http://dx.doi.org/10.1016/j.trstmh.2006.04.001
5. Oudart JL, Rey M. Proteinuria, proteinaemia, and serum transaminase activity in 23 confirmed cases of yellow fever [in French]. Bull World Health Organ. 1970;42:95–102.
6. Francis TI, Moore DL, Edington GM, Smith JA. A clinicopathological study of human yellow fever. Bull World Health Organ. 1972;46:659–67.
7. Jelić O, Fornet-Sapcevski J, Kovacevíc L, Pandak N, Jelić D. Recurrences of viral hepatitis A [in Croatian]. Acta Med Iugosl. 1990;44:565–76.
8. Sook-Hyang Jeong Hyo-Suk Lee. Hepatitis A: clinical manifestations and management. Intervirology. 2010;53:15–19.
9. Sagnelli E, Coppola N, Marrocco C, Onofrio M, Scarano F, Marotta A, et al. HAV replication in acute hepatitis with typical and atypical clinical course. J Med Virol. 2003;71:1–6. http://dx.doi.org/10.1002/jmv.10455

Address for correspondence: Blandine Denis, Hôpital Saint Louis, Service de Maladies Infectieuses et Tropicales, 1 Ave Claude Vellefaux, Paris 75010, France; email: blandine.denis@aphp.fr

Comparative Analysis of Whole-Genome Sequence of African Swine Fever Virus Belgium 2018/1

Jan H. Forth, Marylène Tignon, Ann Brigitte Cay, Leonie F. Forth, Dirk Höper, Sandra Blome, Martin Beer

Author affiliations: Friedrich-Loeffler-Institut, Greifswald, Germany (J.H. Forth, L.F. Forth, D. Höper, S. Blome, M. Beer); Sciensano, Brussels, Belgium (M. Tignon, A.B. Cay)

DOI: https://doi.org/10.3201/eid2506.190286

We analyzed the whole-genome sequence of African swine fever virus Belgium 2018/1. The strain fits into the European genotype II (>99.98% identity). The high-coverage sequence revealed 15 differences compared with an improved African swine fever virus Georgia 2007/1 sequence. However, in the absence of genetic markers, no spatial or temporal correlations could be defined.

African swine fever (ASF) is one of the most pathogenic viral diseases of swine leading to clinical and pathomorphological signs of a viral hemorrhagic fever (*1*). In 2007, ASF was introduced into Georgia (*2*) and thereafter into numerous eastern European and European Union (EU) countries (*3*), as well as Asia (China, Mongolia, and Vietnam) (World Organization for Animal Health–World Animal Health Information database, http://www.oie.int/wahis_2/public/wahid.php/Wahidhome/Home/indexcontent, 2019 Feb 21).

In September 2018, the African swine fever virus (ASFV) was introduced into Belgium (*3*,*4*); as of April 28, 2019, 719 cases have been reported by Belgium's Federal Agency for the Safety of the Food Chain (http://www.afsca.be/ppa/actualite/belgique).

Samples from the first 2 cases were taken for analysis to the Belgium National Reference Laboratory for ASF at Sciensano, Brussels, and were later confirmed by the ASF EU Reference Laboratory (EURL) in Valdeolmos, Spain. Partial sequencing at the EURL revealed a p72 genotype II with CVR-1, IGR-2, and MGF1 variants. Initial assessments of virus type and epidemiology were published by Gariglianey et al. (*4*) to share the data without delay. Subsequently, samples were transferred to the Friedrich-Loeffler-Institut, Greifswald, Germany, for whole-genome sequencing.

We prepared samples and sequenced them on an Illumina MiSeq (https://www.illumina.com), as previously described (*5*). In addition, we enriched DNA libraries for Illumina sequencing for ASFV specific target sequences using an ASFV-specific myBaits kit (Arbor Biosciences, https://arborbiosci.com). We analyzed the resulting sequence data by mapping against an improved ASFV Georgia 2007/1 sequence (International Nucleotide Sequence Database Collaboration accession no. FR682468.2) using Newbler 3.0 software (*6*); we assembled the identified ASFV-specific reads using SPAdes 3.13.0 (*7*).

For the assembly of the inverted terminal repeat (ITR) regions, we mapped the reads against the individual ASFV Georgia 2007/1 ITR regions using Newbler and manually assembled them with the ASFV Belgium 2018/1 sequence in Geneious 11.1.5 (Biomatters, https://www.geneious.com). For validation, we mapped all reads along the final contig using Newbler; the result was a median unique depth of 292 with an interquartile range of 42. We annotated the sequence according to the improved ASFV Georgia 2007/1 sequence, using Glimmer3 in Geneious. We aligned different available ASFV whole-genome sequences using MAFFT 7.388, and we performed a phylogenetic analysis using IQ-TREE v1.6.5 (*8,9*). The whole-genome sequence is available from the International Nucleotide Sequence Database Collaboration databases under study accession no. PRJEB31287 and sequence accession no. LR536725.

The ASFV Belgium 2018/1 whole-genome sequence has a length of 190,599 bp. Comparison with the improved ASFV Georgia 2007/1 sequence revealed 15 differences, for an overall sequence identity of 99.98% at the nucleotide level. The detected differences included 4 nucleotide transitions, 5 nucleotide transversions, 5 changes in homopolymer regions, and 1 integration of a repeat into a previously described variable intergenic region (*10*) (Table).

Altogether, 4 differences in annotated genes are nonsynonymous; 2 cause a frameshift, thereby truncating the MGF 110–1L gene and changing the amino acid sequence of the DP60R protein; and 9 differences were identified in noncoding regions (Table). The differences in the ITR regions must be viewed carefully because of the low coverage in these particular parts of the genome, but the differences in the core regions are well supported by the sequencing data (Table). The differences at the specific positions 7,061; 44,586; 134,524; and 170,827 were also identified in the ASFV-SY2018 (China), Estonia 2014, Kashino 04/13 (Russia), and Pol 16/17 (Poland) sequences, and position 170,827 also in ASFV strain Odintsovo_02/14 (Russia). Further genetic differences could be identified in 7 so-called poly G/C regions. Whether these are artifacts originating from sequencing any of the analyzed genomes or pose real differences remains to be determined by the analysis of further sequences from Belgium and other countries, which is in progress.

Finally, the alignment of all publicly available eastern European whole-genome sequences, as well as ASFV-China, shows that all these genomes are nearly identical with identities of more than 99.9% (Appendix Figure, http://wwwnc.cdc.gov/EID/article/25/6/19-0286-App1.pdf).

In conclusion, we provide a whole-genome analysis of ASFV from Belgium, which could show a high overall identity to recent ASFV strains from eastern Europe and China. We also identified locations showing differences from ASFV Georgia 2007/1 in single nucleotides, as well as a previously described repeat insertion. However, because the low mutation rate and the corresponding high genetic stability of the eastern European ASFV strains have hindered the definition of reliable genetic markers thus far, the currently available whole-genome information does not allow for further statements regarding correlations in space and time, and does not provide enough evidence for a more detailed mapping of strain origin.

Although MGF110 was assigned a possible function in preparing the endoplasmic reticulum for viral morphogenesis (*11*), in the absence of any observations regarding virus attenuation in the field, no conclusion can be drawn on the effect of the observed differences. Therefore, further in vitro and in vivo characterizations using the ASFV Belgium 2018/1 isolate are needed.

In the future, more high-quality whole-genome ASFV sequences might allow identification of genetic markers that could aid high-resolution molecular epidemiology. Coordinated efforts to improve data sharing, together

Table. Differences in the whole-genome sequence of ASFV Belgium2018/1 and the improved ASFV Georgia2007/1 reference genome*

Position	Type	Difference	ASFV Georgia 2007/1†	ASFV Belgium 2018/1†	Coverage	Gene	Synonymous/ nonsynonymous	ORF change
121	Transversion	G121C	AAGAT	AA**C**AT	44	ITR	NA	NA
129	Transversion	A129T	AAATA	AA**T**TA	47	ITR	NA	NA
479	Variation	+T	9 × T	10 × T	767	ITR	NA	NA
1393	Variation	+C	9 × C	10 × C	1375	NA	NA	NA
6786	Variation	–T	9 × T	8 × T	1755	NA	NA	NA
7061	Transition	C7061T	CCCAG	CC**T**AG	1556	MGF 110–1L	Trp197Stop	Shortened by 18 codons
15688	Variation	+3C	17 × C	20 × C	127	MGF 110–13Lb	Frameshift	Enlarged by 1 codon
17640	Variation	+2G	10 × G	12 × G	1117	NA	NA	NA
17854	Variation	+G	9 × G	10 × G	1304	NA	NA	NA
19807	Variation	–G	7 × G	6 × G	1238	NA	NA	NA
20017	Variation	–2G	16 x G	14 × G	832	ASFV G ACD 00350	Frameshift	Truncation
21815	Variation	+2G	9 × G	11 × G	1184	NA	NA	NA
27439	Variation	–T	10 × T	9 × T	1895	NA	NA	NA
44586	Transition	A44586G	TGAAA	TG**G**AA	1292	MGF 505–9R	Lys323Glu	NA
73282	Variation	–T	9 × T	8 × T	1241	NA	NA	NA
134524	Transition	T134524C	CATTT	CA**C**TT	1665	NP419L	Asp414Ser	NA
145080	Transition	G145080A	GAGGC	GA**A**GC	1266	D117L	Pro84Leu	NA
170827	Transversion	T170827A	GATGG	GA**A**GG	1263	I267L	Ile195Phe	NA
190138	Variation	+A	9 × A	10 × A	3021	DP60R	Frameshift	22 changed codons
173402	Repeat integration	+TATATAG GAA	NA	+TATATAGG AA	1731	NA	NA	NA
190478	Transversion	T190478A	TATTT	TA**A**TT	49	ITR	NA	NA
190486	Transversion	C190486G	ATCTT	AT**G**TT	49	ITR	NA	NA

*Differences are show in bold and underlined. ASFV, African swine fever virus; ITR, inverted terminal repeat; NA, not applicable; ORF, open reading frame.
†International Nucleotide Sequence Database Collaboration accession nos: ASFV Georgia 2007/1, FR682468.2; ASFV Belgium 2018/1, LR536725.

with harmonized protocols under quality assurance, are of utmost importance to interpret results correctly and aid the fight against ASF.

Acknowledgments

The authors thank Patrick Zitzow for excellent technical assistance. The rapid and efficient support from the EURL (M. Arias, Valdeolmos, Spain) was highly appreciated. The authors from Belgium also thank the excellent collaboration with the Walloon Region.

Dr. Forth is a biologist and postdoctoral researcher at the Friedrich-Loeffler-Institut, Greifswald, Germany. His work focuses mainly on ASFV whole-genome sequencing, molecular epidemiology, and virus evolution.

References

1. Alonso C, Borca M, Dixon L, Revilla Y, Rodriguez F, Escribano JM; ICTV Report Consortium. ICTV virus taxonomy profile: Asfarviridae. J Gen Virol. 2018;99:613–4. http://dx.doi.org/10.1099/jgv.0.001049
2. Beltran-Alcrudo D, Lubroth J, Depner K, De La Rocque S. African swine fever in the Caucasus. FAO EMPRES Watch. 2008:1–8 [cited 2019 Mar 22]. http://www.fao.org/docs/eims/upload/242232/ew_caucasus_apr08.pdf</eref>
3. Linden A, Licoppe A, Volpe R, Paternostre J, Lesenfants C, Cassart D, et al. Summer 2018: African swine fever virus hits north-western Europe. Transbound Emerg Dis. 2019;66:54–5. http://dx.doi.org/10.1111/tbed.13047
4. Garigliany M, Desmecht D, Tignon M, Cassart D, Lesenfant C, Paternostre J, et al. Phylogeographic analysis of African swine fever virus, Western Europe, 2018. Emerg Infect Dis. 2019;25:184–6. http://dx.doi.org/10.3201/eid2501.181535
5. Wylezich C, Papa A, Beer M, Höper D. A Versatile sample processing workflow for metagenomic pathogen detection. Sci Rep. 2018;8:13108. http://dx.doi.org/10.1038/s41598-018-31496-1
6. Margulies M, Egholm M, Altman WE, Attiya S, Bader JS, Bemben LA, et al. Genome sequencing in microfabricated high-density picolitre reactors. Nature. 2005;437:376–80. http://dx.doi.org/10.1038/nature03959
7. Antipov D, Korobeynikov A, McLean JS, Pevzner PA. hybridSPAdes: an algorithm for hybrid assembly of short and long reads. Bioinformatics. 2016;32:1009–15. http://dx.doi.org/10.1093/bioinformatics/btv688
8. Nguyen L-T, Schmidt HA, von Haeseler A, Minh BQ. IQ-TREE: a fast and effective stochastic algorithm for estimating maximum-likelihood phylogenies. Mol Biol Evol. 2015;32:268–74. http://dx.doi.org/10.1093/molbev/msu300
9. Kalyaanamoorthy S, Minh BQ, Wong TKF, von Haeseler A, Jermiin LS. ModelFinder: fast model selection for accurate phylogenetic estimates. Nat Methods. 2017;14:587–9. http://dx.doi.org/10.1038/nmeth.4285
10. Goller KV, Malogolovkin AS, Katorkin S, Kolbasov D, Titov I, Höper D, et al. Tandem repeat insertion in African swine fever virus, Russia, 2012. Emerg Infect Dis. 2015;21:731–2. http://dx.doi.org/10.3201/eid2104.141792
11. Netherton C, Rouiller I, Wileman T. The subcellular distribution of multigene family 110 proteins of African swine fever virus is

determined by differences in C-terminal KDEL endoplasmic reticulum retention motifs. J Virol. 2004;78:3710–21. http://dx.doi.org/10.1128/JVI.78.7.3710-3721.2004

Address for correspondence: Martin Beer, Institute of Diagnostic Virology, Friedrich-Loeffler-Institut, Südufer 10, 17489 Greifswald, Germany; email: martin.beer@fli.de

Highly Pathogenic Swine Getah Virus in Blue Foxes, Eastern China, 2017

Ning Shi, Li-Xia Li, Rong-Guang Lu, Xi-Jun Yan, Hao Liu

Author affiliations: Foshan University, Foshan, China (N. Shi, H. Liu); Jilin Wildlife Rescue and Rehabilitation Center, Forestry Department of Jilin Province, Changchun, China (L.-X. Li); Chinese Academy of Agricultural Sciences, Changchun (R.-G. Lu, X.-J. Yan)

DOI: https://doi.org/10.3201/eid2506.181983

We isolated Getah virus from infected foxes in Shandong Province, eastern China. We sequenced the complete Getah virus genome, and phylogenetic analysis revealed a close relationship with a highly pathogenic swine epidemic strain in China. Epidemiologic investigation showed that pigs might play a pivotal role in disease transmission to foxes.

Getah virus (GETV; genus *Alphavirus*, family *Togaviridae*) is a mosquitoborne RNA virus that causes death in young piglets, miscarriage in pregnant sows, and mild illness in horses (*1–3*). Serologic surveys show that the infection might occur in cattle, ducks, and chickens (*4*); some evidence suggests that GETV can infect humans and cause mild fever (*5,6*).

In September 2017, twenty-five 5-month-old blue foxes at a farm in Shandong Province in eastern China showed symptoms of sudden fever, anorexia, and depression; 6 of the 25 animals had onset of neurologic symptoms and died on the third day of illness. We collected blood samples from 45 healthy and 25 ill foxes. We subjected the tissue samples from dead animals, including the brains, lungs, spleens, kidneys, livers, intestines, hearts, and stomachs, to hematoxylin and eosin staining. Microscopic examination confirmed the presence of typical lesions in cerebral cortices with mild neuronal degeneration and inflammatory cell infiltration in vessels, as well as severe hemorrhagic pneumonia, congestion, and hemorrhage with a large number of erythrocytes in the alveolar space (Figure) (*1*). No obvious lesions were found in other organs.

We used supernatants of homogenized brain and lung tissues from each dead fox to inoculate Vero cells, as described previously (*7*). We observed a cytopathogenic effect within 72 hours. We observed numerous spherical, enveloped viral particles, ≈70 nm in diameter, after negative staining in a transmission electron microscope. To identify potential viral pathogens, we performed reverse transcription PCR (RT-PCR) to detect a panel of viruses, including canine distemper virus, canine parvovirus, canine coronavirus, and canine adenovirus. However, we detected none of these classical endemic viruses.

During the investigation, farmers reported that the foxes had been fed on organs from symptomatic pigs. We therefore tested for the presence of African swine fever virus, pseudorabies virus, porcine reproductive and respiratory syndrome virus, classical swine fever virus, Japanese encephalitis virus, porcine circovirus type 2, porcine circovirus type 3, porcine cytomegalovirus, and alphavirus by using the primers for those viruses (Appendix Table 2, https://wwwnc.cdc.gov/EID/article/25/6/18-1983-App1.pdf). RT-PCR using universal primers for alphavirus (M2w-cMw3) produced a 434-bp amplicon when we tested all samples from dead foxes. Sanger sequencing of the amplicon and a BLAST search (https://blast.ncbi.nlm.nih.gov/Blast.cgi) identified the sequence as that of GETV.

To further investigate the epidemic GETV infection, we performed quantitative RT-PCR by using RNA from all fox samples, as described elsewhere (*7*). Lung samples from all 6 dead foxes were positive, whereas only 2 samples from the remaining 19 ill foxes were also positive. None of the samples from healthy foxes were positive (Appendix Tables 1, 3). We measured serologic neutralizing antibodies by using a GETV isolate from a symptomatic fox, as previously described (*8,9*). Results showed no neutralizing antibody (<1:2) in healthy blue foxes (group 1) and variable levels of neutralizing antibodies (1:2 to 1:256) in ill foxes (groups 2–4) (Appendix Table 3). Samples from ill foxes with lower antibody titers had higher copies of RNA (groups 2–4). Spearman correlation analysis revealed a significant negative correlation between antibody titers and viral RNA copy numbers ($r^2 = 0.952$; $p<0.01$).

We obtained the complete genome of the novel GETV SD1709 strain (GenBank accession no. MH106780) by using a conventional RT-PCR method (*10*). SD1709 genome sequence comparisons showed high identity with the porcine GETV strain (HuN1) at the nucleotide (99.6%) and deduced amino acid (99.7%–99.8%) sequences (Appendix Table 4). Furthermore, phylogenetic analysis of the

Article DOI: https://doi.org/10.3201/eid2506.190286

Comparative Analysis of Whole-Genome Sequence of African Swine Fever Virus Belgium 2018/1

Appendix

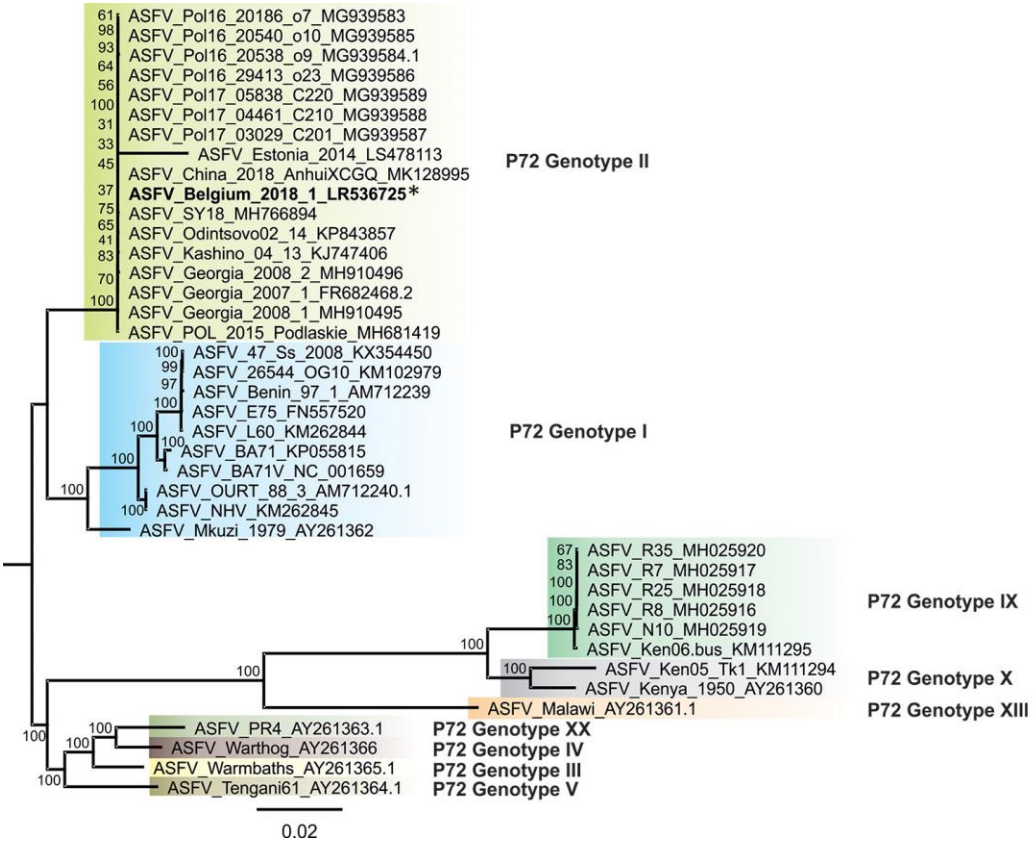

Appendix Figure. Phylogenetic tree of all available African swine fever virus (ASFV) whole-genome sequences. We constructed a maximum-likelihood tree using IQ-TREE v1.6.5 (www.iqtree.org) with standard model selection, resulting in the best-fit model K3Pu+F+R3 (3 substitution types model + empirical base frequencies + FreeRate model with 3 categories) based on MAFFT v7.388 (https://mafft.cbrc.jp) aligned ASFV whole-genome sequences. Statistical support of 10,000 ultrafast bootstraps is indicated at the nodes. Taxon names include, where available, ASFV designation and International Nucleotide Sequence Database Collaboration accession number. Numbers along branches are bootstrap values. Scale bar represents nucleotide substitutions per site. Colors indicate specific genotypes; * indicates the genome discussed in this study.